Applied Catalysis B: Environmental 126 (2012) 100–107

Contents lists available at SciVerse ScienceDirect

Applied Catalysis B: Environmental

journal homepage: www.elsevier.com/locate/apcatb

Role of activated carbon in the photocatalytic degradation of 2,4-dichlorophenoxyacetic acid by the UV/TiO_2/activated carbon system

J. Rivera-Utrilla*, M. Sánchez-Polo, M.M. Abdel daiem, R. Ocampo-Pérez

Department of Inorganic Chemistry, Faculty of Science, University of Granada, 18071, Granada, Spain

ARTICLE INFO

Article history:
Received 24 May 2012
Received in revised form 12 July 2012
Accepted 16 July 2012
Available online 24 July 2012

Keywords:
2,4-Dichlorophenoxyacetic acid
Photodegradation
Titanium dioxide
Ozonated activated carbon

ABSTRACT

The objective of this study was to photocatalytically degrade the pesticide 2,4-dichlorophenoxyacetic acid (2,4-D) by using the integrated UV/TiO_2/activated carbon system and to study the degradation kinetics and the role of the chemical and textural properties of activated carbon in this process. Results obtained show that the presence of activated carbon during the catalytic photodegradation (UV/TiO_2) of 2,4-D considerably increases its percentage removal. After 60 min of treatment, the highest percentage 2,4-D degradation is obtained in the presence of the activated carbons with the greatest content of carboxyl groups. In order to determine the role of activated carbon in this process, we determined the adsorptive and photocatalytic contribution (UV/TiO_2) to the overall 2,4-D removal. The total percentage removal by the UV/TiO_2/activated carbon system is much higher than the value obtained by summing the adsorptive and catalytic contributions, mainly when the carbon has an elevated carboxyl group content. No relationship was observed between the textural properties of activated carbons and their synergistic activity; however, the carbons with the greatest carboxyl group content showed the highest synergistic activity. Together with the results of chemical and superficial characterization of the carbon samples after their utilization in the photocatalytic process (UV/TiO_2), these findings demonstrate that the reduction of superficial carboxyl groups to alcohol groups is the main pathway by which activated carbon enhances the additional generation of $HO^\bullet$ radicals in the medium. Experiments conducted in the presence of radical scavengers (carbonate ions, sulfate ions, and *t*-butanol) revealed that $H^\bullet$, e_{aq}^-, and $HO^\bullet$ species participate in the 2,4-D photodegradation. According to the time course of total organic carbon and toxicity during 2,4-D photodegradation, its complete mineralization is not achieved, and the toxicity of the degradation compounds is lower than that of 2,4-D.

1. Introduction

In general, polluted waters are effectively treated by biological treatment plants using adsorbents or conventional chemical processes (chlorination, ozonation, or oxidation with permanganate). However, these procedures are occasionally unable to degrade the pollutants present to the levels required by law and for subsequent use of the effluent. Over the past few years, new technologies have been developed, known as advanced oxidation processes (AOPs), which have proven highly effective in the oxidation of numerous organic and inorganic compounds. The mechanism underlying all of these processes is the generation of free radicals, especially the hydroxyl radical ($HO^\bullet$) [1].

An alternative to the generation of free radicals is photocatalysis on the surface of a semiconductor. Heterogeneous photocatalysis consists of the direct or indirect absorption of visible or ultraviolet (UV) radiant energy by a solid that, in its excited form, acts as a catalyst for degradation reactions with compounds at the solid–liquid interface. Various semiconductor materials possess suitable characteristics for their utilization as photocatalysts, i.e., stability, economically affordability and no requirement for excessively energetic radiation, and those that are activated by the radiation of the visible spectrum are of particular interest. The literature includes studies of photocatalysts such as TiO_2, ZnO, SnO_2, WO_3, ZrO_2, CeO_2, CdS, and Fe oxides, which have all evidenced a good performance in the removal of numerous pollutants [2–7].

It was recently reported that carbon materials can markedly improve the photocatalytic process, largely through one of the three following mechanisms: (i) minimization of the recombination of photogenerated electron–hole pairs; (ii) modification of the band gap of the photocatalyst to higher wavelengths; and (iii) presence of adsorption centers that accelerate contact between pollutant and catalyst [8–15].

Various researchers have reported a clear correlation between the photocatalytic activity of carbon/TiO_2 composites and the chemical and textural properties of the activated carbon (AC) used

* Corresponding author. Tel.: +34 958248523; fax: +34 958248526.
E-mail address: jrivera@ugr.es (J. Rivera-Utrilla).

0926-3373/$ – see front matter © 2012 Elsevier B.V. All rights reserved.
http://dx.doi.org/10.1016/j.apcatb.2012.07.015

as support [16]. The variation in degradation rate as a function of the properties of the carbon material has been described as a synergistic effect in the literature. Thus, Matos et al. [16] studied the photocatalytic degradation of phenol, 4-chlorophenol, and 2,4-D in the presence of TiO_2 and two commercial activated carbons (L and H) and found that the presence of carbon H improved the photocatalytic degradation of pollutants with a synergistic factor of 2.5, 2.4, and 1.3, respectively. Cordero et al. [17] used a carbon prepared from *Tabebuia pentaphyla* wood and activated with CO_2 at 450–1000 °C and reported that it exerted a synergistic effect on the catalytic activity of TiO_2, enhancing the degradation of 4-chlorophenol.

A possible mechanism by which activated carbon increases the photocatalytic activity of TiO_2 was proposed by Silva and Faria [10], who reported that the presence of mild concentrations of oxygen-containing surface groups, mainly carboxylic acids and phenols, may improve the photocatalytic activity of multi-walled carbon nanotubes–TiO_2 composite catalysts in the photocatalytic oxidation of benzene derivatives in aqueous suspensions.

In a previous study, Ocampo-Pérez et al. [8] investigated the photocatalytic degradation of cytarabine in aqueous phase (UV/TiO_2) in the presence of activated carbon with different chemical and textural properties. Results obtained suggested that the reaction of e_{aq}^-, from the UV–TiO_2 interaction, with the activated carbon carboxylic acids are responsible for the increased photocatalytic activity of TiO_2. We therefore hypothesized that the interaction between e_{aq}^- and surface carboxylic acids on oxidized carbons reduces carboxylic acids to aldehydes, generating H_2O_2 that can be decomposed into HO• radicals, and that these aldehydes can be transformed into a surface alcohol group that generates additional HO• radicals. The proposed mechanism is given by the following reactions.

$$AC - COOH + H_2O \xrightarrow{e_{aq}^-} AC - COH + H_2O_2 \quad (1)$$

$$H_2O_2 + h\nu(UV) \rightarrow 2HO^\bullet \quad (2)$$

$$AC - COH + 2H_2O \xrightarrow{2e_{aq}^-} AC - CH_2OH + 2HO^\bullet \quad (3)$$

With this background, the main aim of the present study was to experimentally confirm this mechanism, thereby advancing knowledge of the UV/TiO_2/activated carbon system and assisting selection of the most appropriate carbons for obtaining the maximum degradation and mineralization of pollutants. For this purpose, we photocatalytically degraded herbicide 2,4-D, selected as model compound, using the UV/TiO_2/activated carbon system and determined the degradation kinetics, the influence of operational variables, the effect of the chemical nature of the carbon, and the modifications of the carbon surface chemistry during the photooxidation process.

2,4-D is a herbicide in extensive use worldwide [18], thanks to its low cost and good selectivity [19], and it has been detected in waters in various regions [20]. It is considered moderately toxic, with a maximum allowed concentration in drinking water of 100 μg/L. 2,4-D has been eliminated from aqueous solutions with varying degrees of success by means of microbial, chemical, and photochemical processes [21,22]. Photocatalysis has been reported as a good alternative for the degradation of recalcitrant compounds [23] and represents another potential technology for removing 2,4-D.

2. Experimental method

2.1. Reagents

All chemical reagents used in this study (2,4-D, acetonitrile, *t*-butanol, sodium sulfate, and sodium carbonate) were high-purity analytical grade reagents supplied by Sigma–Aldrich. All solutions were prepared with ultrapure water obtained from Milli-Q® equipment (Millipore). Fig. 1 depicts the molecular structure of 2,4-D and the species diagram of 2,4-D as a function of pH.

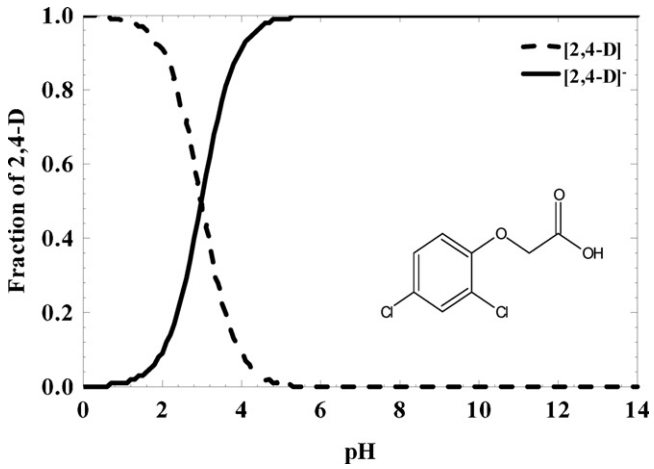

Fig. 1. Molecular structure and species diagram of 2,4-D as a function of pH.

2.2. Activated carbons

Three commercial powdered activated carbons were used: Sorbo (S), Merck (M), and Witcot (W). The particle size range was 0.05–0.08 mm. Activated carbon W was oxidized with ozone (W_{O3}) in an OZOKAV ozonator with a maximum capacity of 76 mg/min, placing 0.50 g of activated carbon W in a column with upward O_3 flow and keeping the activated carbon in suspension to ensure its homogeneous oxidation. Two carbon samples were obtained after ozone exposure of 30 min (W_{O3-30}) and 120 min (W_{O3-120}). All activated carbon samples were stored in a sealed container and placed in an oven at 110 °C before their use.

The physical characterization (surface area from adsorption of N_2 at 77 K) and chemical characterization (functional groups and pH of the point of zero charge) of the five carbon samples were previously reported [8], and some of these characteristics are given in Table 1.

After the photocatalytic process, the carbon samples were again physically and chemically characterized to determine the chemical changes undergone by the activated carbons during 2,4-D degradation by the UV/TiO_2/activated carbon system. A detailed description of the characterization methods was previously published [8,24,25].

2.3. Titanium dioxide

TiO_2 used in this study was supplied by Degussa. X-ray diffraction (XRD) analysis revealed 93% anatase content and 7% rutile content. The surface area of TiO_2 was 60.9 m^2/g. After the photocatalysis, the TiO_2 sample was again analyzed by XRD in order to determine changes in its crystal structure.

2.4. Adsorption isotherms of 2,4-D on both activated carbon and TiO_2

The experimental data for the adsorption equilibrium of 2,4-D on activated carbon or TiO_2 were obtained as follows. A mass of 10 mg of activated carbon or TiO_2 and 30 mL of 2,4-D solution at T = 25 °C and pH 7 were added in the batch adsorber; the 2,4-D solution, at initial 2,4-D concentrations of 10–100 mg/L, remained in contact with the activated carbon or TiO_2 particles until

Table 1
Textural and chemical characteristics of the activated carbons.

Activated carbon	S_{BET} [a] (m^2/g)	pH_{PZC} [b]	Basic groups (mequiv./g)	Carboxyl groups (mequiv./g)	Phenol groups (mequiv./g)	Lactone groups (mequiv./g)	Total acid groups (mequiv./g)
S	1225	10	1.08	0.00	0.24	0.060	0.30
M	1301	7.7	0.44	0.04	0.16	0.120	0.32
W	1110	6.5	0.76	0.32	0.42	0.035	0.78
W_{O3-30}	670	3.3	0.05	1.42	0.15	0.99	2.56
W_{O3-120}	655	2.9	0.03	1.55	0.11	1.86	3.52

[a] Surface area.
[b] pH of the point of zero charge.

equilibrium was reached. Preliminary experiments revealed that two days were sufficient to attain equilibrium. After reaching equilibrium, the solutions were centrifuged and filtered with Millipore disc filters (0.2 μm) to remove activated carbon or TiO_2, and the final 2,4-D concentration was determined. The mass of 2,4-D adsorbed at equilibrium was calculated by a mass balance method.

2.5. Photoreactor design

2,4-D degradation experiments in the presence of activated carbon and/or TiO_2 were conducted in a photoreactor formed by concentric tubes: a stainless steel outer tube (inner diameter [i.d.] of 13 cm × height of 18 cm) and quartz inner tube (i.d. of 5.5 cm × height of 45 cm). The inner tube contained a low-pressure Hg lamp (Heraeus Noblelight model TNN 15/32, nominal power 15 W, $I_0 = 1.027 \times 10^{-4}$ Einstein s^{-1} m^{-2} at $\lambda = 254$ nm). The annular space of the photoreactor contained a sample holder with a capacity for six quartz reaction tubes (i.d. of 1.6 cm × height of 20 cm). Solutions in reaction tubes were kept at constant temperature by using a Frigiterm ultrathermostat, and the suspension within reaction tubes was maintained in agitation by means of a magnetic agitation system.

2.6. Photocatalytic degradation of 2,4-D in the presence of activated carbon and/or TiO_2

Experimental 2,4-D photodegradation data were obtained as follows. A concentrated solution of 2,4-D (1000 mg/L) was prepared by adding 0.1 g of 2,4-D to a 100 mL flask with ultrapure water; 28.5 mL of ultrapure water were placed in the reaction tubes and different masses of activated carbon and TiO_2 were added. The suspension was homogenized by manual agitation and placed inside the photoreactor, where agitation continued. An aliquot (1.5, 0.75, or 0.30 mL) of 2.4-D solution was added to the reaction tubes to obtain an initial 2,4-D concentration of 50, 25, or 10 mg/L, respectively, simultaneously activating the photoreactor lamp. For all experiments the solutions were in anoxic conditions which were achieved by bubbling N_2, and the solution pH was 7. Photocatalytic degradation of 2,4-D was monitored by taking 1.0 mL samples at regular time intervals for 2,4-D concentration measurement. After samples were withdrawn, they were immediately filtered with Millipore disc filters (0.20 μm- GSWP) to remove the activated carbon and TiO_2.

Photocatalytic degradation of 2,4-D in the presence of radical scavengers was carried out using the same methodology but adding an aliquot of *t*-BuOH, Na_2SO_4, or Na_2CO_3/Na_2SO_4 solutions to reaction tubes to obtain the desired concentration of 1 M of each radical scavenger.

2.7. Determination of 2,4-D concentration in aqueous solution

The 2,4-D concentration in aqueous solution was determined by reverse-phase high performance liquid chromatography (HPLC) using a liquid chromatograph (Thermo-Fisher) equipped with a visible UV detector and an autosampler with capacity for 120 vials. A Nova-Pak® C_{18} chromatographic column was used (4 μm particle size; 3.9 × 150 mm). The mobile phase was 20% acetonitrile and 80% water in isocratic mode at a flow of 1.0 mL/min; the detector wavelength was 280 nm, and the injection volume was 100 μL.

2.8. Determination of total organic carbon

Total organic carbon (TOC) present in the system was determined by using a Shimadzu V-CSH analyzer with ASI-V autosampler.

2.9. Determination of degradation byproduct toxicity

Degradation byproduct toxicity was determined by using the LUMIStox 300 system and LUMISTherm incubator (Dr. LangeGmbH), based on the normalized biotest (UNE/EN/ISO 11348-2) of luminescent inhibition of Vibrio Fischeri bacteria (NRRL B-11177) [26,27]. Toxicity was expressed as percentage inhibition at 15 min of exposure with reference to a stock saline solution (control).

3. Results and discussion

3.1. Adsorption isotherms and adsorption kinetics of 2,4-D on activated carbon

We first determined the adsorptive capacity of the activated carbons to enable subsequent interpretation of the results of catalytic photooxidation of 2,4-D in their presence. Fig. 2a depicts the adsorption isotherms of 2,4-D on the five carbon samples.

The experimental data were interpreted with the Langmuir adsorption isotherm, which is mathematically represented as follows:

$$q = \frac{q_m K C_e}{1 + K C_e} \quad (4)$$

where C_e is 2,4-D concentration at equilibrium (mg/L), q is the mass of 2,4-D adsorbed per mass unit of carbon (mg/g), q_m is the maximum amount of 2.4-D adsorbed per adsorbent mass unit (mg/g), and K is the Langmuir constant (L/mg).

Table 2 lists the values of the above parameters and the percentage mean absolute deviation, %*D*, which was estimated from the following equation:

$$\%D = \frac{1}{N}\sum_{i=1}^{N}\left|\frac{q_{exp} - q_{pred}}{q_{exp}}\right| \times 100\% \quad (5)$$

where N is the number of experimental data points, q_{exp} (mg/g) is the experimental mass of 2,4-D adsorbed, and q_{pred} (mg/g) is the mass of adsorbed 2,4-D predicted with the Langmuir adsorption isotherm.

According to the data in Table 2, the highest adsorption capacity was obtained with sample S, followed by samples M, W, W_{O3-30},

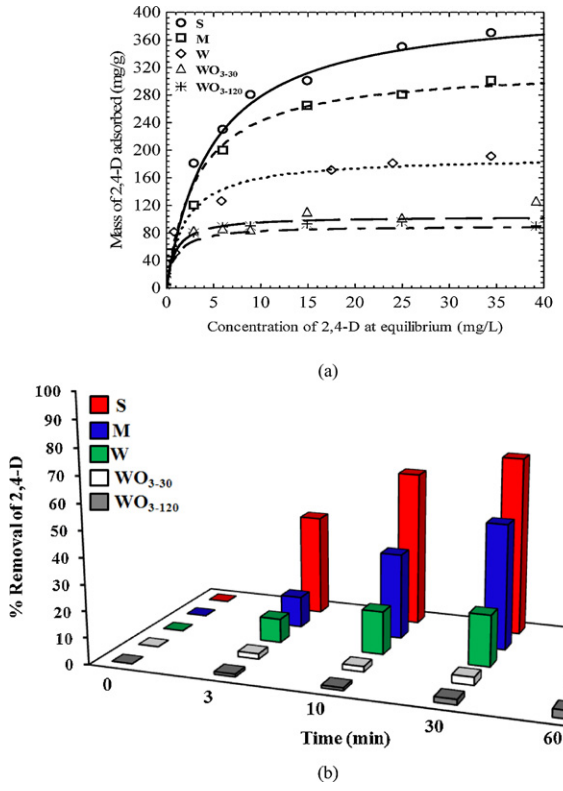

Fig. 2. Adsorption of 2,4-D on activated carbons, (a) adsorption isotherms, (b) adsorption kinetics. $T = 25^{\circ}$ C and pH 7.

and W_{O3-120}, with q_m values ranging from 412.1 mg/g (sample S) to 90.3 mg/g (sample W_{O3-120}). The low adsorption capacity of ozonated carbons W_{O3-30} and W_{O3-120} is explained by two factors: (a) under the experimental conditions used in this study (pH 7, $T = 25\,^{\circ}C$), there is an increase in repulsive electrostatic interactions between 2,4-D and carbon surface, because 2,4-D is in deprotonated form (Fig. 1) with a negative charge ($pK_a = 2.85$) and the carbon surface is negative ($pH_{solution} > pH_{PZC}$) and becomes more negative with lower pH_{pcz} (Table 1); and (b) oxidation of the activated carbons increases the number of surface carboxyl groups (electronic deactivators of aromatic rings) and reduces the concentration of phenol groups (electronic activators of these rings), weakening $\pi - \pi$ adsorbate–adsorbent dispersion interactions through a reduction in the electronic density of carbon graphene planes [28–31].

Fig. 2b shows the percentage 2,4-D removal as a function of time over a 60 min contact period with the different activated carbons at an initial 2,4-D concentration of 50 mg/L and carbon mass of 10 mg. This figure demonstrates that the percentage 2,4-D removal markedly increased after longer contact times with carbons S, M, and W and remains almost constant over time with samples W_{O3-30} and W_{O3-120}. After 60 min of contact, the highest percentage removal (72%) was with carbon S, followed by carbons M (56%), W (23%), W_{O3-30} (3%), and W_{O3-120} (4%). Hence, carbon S has the highest adsorption capacity and removal rate. It should be noted that the adsorption rate of organic compounds on granular activated carbon is generally controlled by intraparticle diffusion (diffusion in pore volume or superficial diffusion) [32,33]; however, external mass transport was more important in the present study, in which a very small particle size (0.05–0.08 mm) was used in order to achieve a maximum reduction in diffusion effects, considerably reducing the intraparticle trajectory of 2,4-D molecules.

Table 2
Results obtained by applying the Langmuir equation to the equilibrium adsorption data.

Activated carbon	q_m (mg/g)	K (L/mg)	%D
S	412.1	0.207	11.1
M	321.1	0.307	3.1
W	190.8	0.507	5.1
W_{O3-30}	104.1	1.074	14.5
W_{O3-120}	90.3	1.074	8.2

3.2. Photocatalytic degradation of 2,4-D in the presence of the activated carbons

Fig. 3a depicts the variation in percentage 2,4-D degradation as a function of treatment time with the UV/TiO_2 system in the presence of carbons S, M, and W, while Fig. 3b depicts this variation in the presence of carbons W_{O3-30} and W_{O3-120}. Fig. 3a shows that the highest percentage 2,4-D removal after 60 min of treatment was obtained with carbon S (80%), followed by carbons M (72%) and W (59%). Comparing with the results in Fig. 2b, the removal of 2,4-D was 1.1, 1.38, and 2.57-fold higher, respectively, with the combined UV/TiO_2/activated carbon process than with the adsorption process. The role of activated carbon in the UV/TiO_2/activated carbon system was analyzed by determining the contributions of adsorption and photocatalysis (UV/TiO_2) to the removal of 2,4-D at 60 min of the combined treatment. The results in Table 3 show that: (i) the greatest adsorptive contribution to the global removal process is made with carbons S and M; (ii) with these two carbons (S and M), the contribution of the photocatalytic process (UV/TiO_2) is very low in comparison to the contribution of the adsorptive process, and (iii) with carbon W, the total percentage removal obtained by the UV/TiO_2/activated carbon system is markedly higher than the result of summing the adsorptive and catalytic contributions,

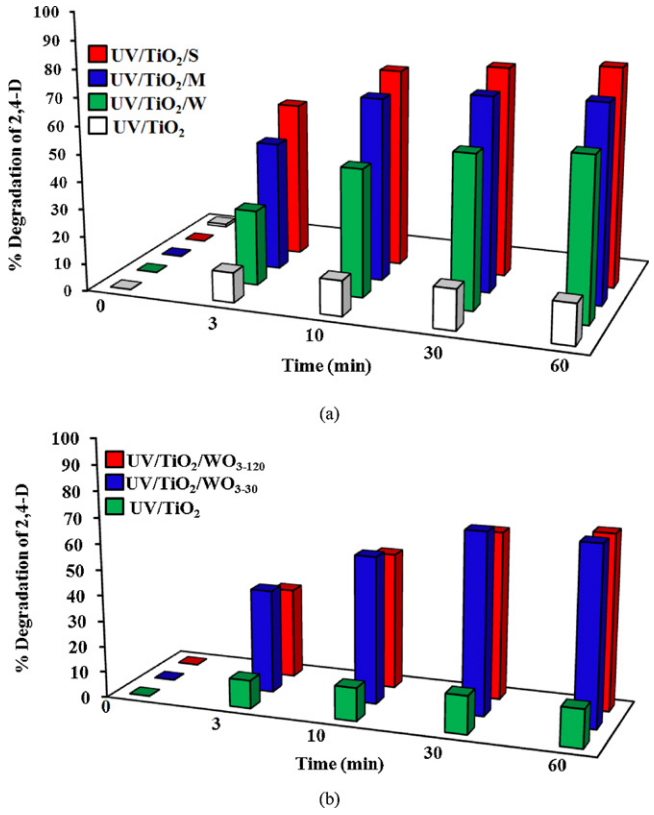

Fig. 3. 2,4-D photodegradation by means of the UV/TiO_2 system in the presence of different activated carbons. $T = 25\,^{\circ}C$, pH 7, [2,4-D] = 50 mg/L, mass of TiO_2 and activated carbon = 5 mg, and $V = 30$ mL.

Table 3
Adsorptive and photocatalytic contributions to the removal of 2,4-D with the UV/TiO_2/activated carbon system.

Activated carbon	Total (%)	Adsorption (%)	UV/TiO_2 (%)	Synergistic contribution (%)
S	80	72	14	0
M	72	56	14	2
W	59	23	14	22
W_{O3-30}	70	3	14	53
W_{O3-120}	70	4	14	52

indicating that its presence has a synergistic effect on the 2,4-D removal process.

The results in Table 3 were compared with the chemical and textural properties of the activated carbons. No clear relationship was observed between the surface area and the synergistic contribution to the global removal process, given that the three activated carbons have a similar surface area (≅1200 m^2/g). However, the content of carboxyl and phenol groups is higher in carbon W than in carbons S or M (Table 1). Hence, the synergistic activity of carbon W in the removal of 2,4-D by the UV/TiO_2/activated carbon system may be related to the elevated carboxyl group content on its surface (0.32 mequiv./g vs. 0.00 mequiv./g on carbon S and 0.04 mequiv./g on carbon M), as proposed in a previous study [8].

The role of carboxyl groups in the photocatalytic process was examined by increasing the carboxyl group content of carbon W through oxidation with ozone for 30 min (W_{O3-30}) and 120 min (W_{O3-120}) and then texturally and chemically characterizing these samples (Table 1). The ozone treatment reduced the surface area value by 50%, increased the content of carboxyl and lactone groups, and reduced the content of phenol groups. The mechanism by which ozone interacts with the activated carbon surface has been reported in various publications [25,34].

Fig. 3b depicts the photocatalytic degradation of 2,4-D in the presence of these ozonated samples (W_{O3-30} and W_{O3-120}), demonstrating that the degradation was markedly enhanced by their presence, achieving 70% removal of 2,4-D after 60 min in both cases. This is much higher than the percentage removal obtained with the untreated carbon (W). As shown in Table 3, (i) these ozonated carbon samples (W_{O3-30} and W_{O3-120}) make a very low adsorptive contribution (<4%) to the global 2,4-D removal process, and (ii) they make the highest synergistic contribution to this global process (>50%).

In order to identify the mechanism by which ozonated carbon samples enhance 2,4-D photocatalysis, we chemically characterized sample W_{O3-30} by exposing it to UV and UV/TiO_2 radiation in the absence of 2,4-D. The results in Table 4 shows: (i) similar values of surface acid groups between UV-treated and untreated samples, and (ii) a lower concentration of carboxyl groups and markedly higher content of phenol and lactone groups in the UV/TiO_2-treated vs. untreated samples.

These results verify the proposed mechanism (reactions (1)–(3)), indicating that the main pathway by which activated carbons enhance 2,4-D removal by the UV/TiO_2/carbon system is the reduction of superficial carboxyl groups to aldehyde groups and finally to alcohol groups. Alcohol groups formed on the carbon surface may in turn react with adjacent carboxyl groups in the graphene planes of the activated carbon, generating lactone groups. This would explain the increase in lactone groups in sample W_{O3-30} with the UV/TiO_2/W_{O3-30} system. The increase in phenol groups in sample W_{O3-30} would result from the decarboxylation of carboxyl groups to CO_2 by $HO^\bullet$ radicals, followed by oxidation of the nascent surface carbons to phenol groups.

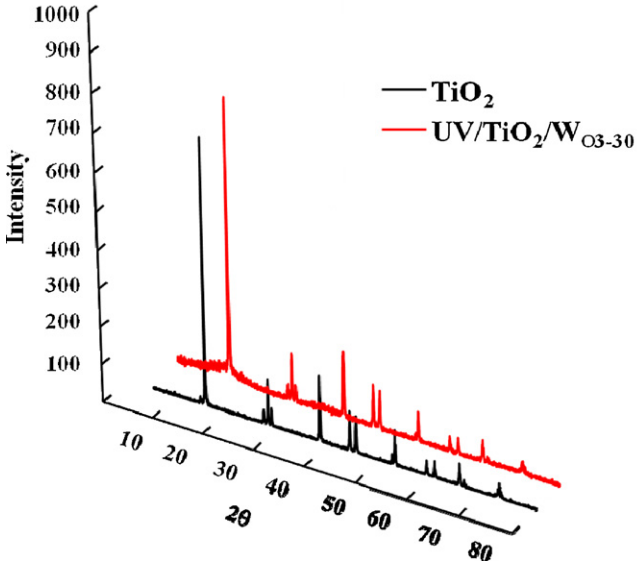

Fig. 4. XRD of TiO_2 before and after treatment.

Fig. 4 depicts the results from XRD analysis of the crystallinity of TiO_2 before and after photocatalysis. The crystallinity phases (anatase and rutile) were computed by using the following equation [35]

$$R(T) = 0.679\left(\frac{I_R}{I_R + I_A}\right) + 0.312\left(\frac{I_R}{I_R + I_A}\right)^2 \quad (6)$$

where $R(T)$ is the rutile percentage, I_A is the intensity of the main anatase peak ($2\theta = 25.30^\circ$), and I_R is the intensity of the main rutile peak ($2\theta = 27.44^\circ$). The content of both samples was 93% anatase and 7% rutile. Hence, the crystallinity of TiO_2 is not modified by interactions between the species generated in TiO_2 photoactivation and the acid sites on the activated carbon.

The 2,4-D degradation by-products obtained by using both UV/TiO_2 and UV/TiO_2/W_{O3-30} systems were determined by means of a ultra-pressure liquid chromatograph (UPLC) coupled to a mass spectrometer. In both cases the by-products detected were: 2-(4-chloro-2-hydroxyphenoxy)acetic acid, 2-(2,4-dihydroxyphenoxy)acetic acid, 5-chloro-2-methylphenol, and 4-ethoxybenzene-1,3-diol.

3.3. *Effect of the mass of activated carbon and TiO_2 on 2,4-D photocatalytic degradation*

The effect of the mass of TiO_2 and activated carbon on the percentage 2,4-D degradation was assessed by using a three-level full factorial design with one center point. A total of 9 experiments were generated, taking the percentage degradation as response and the

Table 4
Chemical characteristics of the W_{O3-30} sample after treatment with UV or UV/TiO_2.

Activated carbontreatment	pH_{PZC}	Basic groups (mequiv./g)	Carboxyl groups (mequiv./g)	Phenol groups (mequiv./g)	Lactone groups (mequiv./g)	Acid groups (mequiv./g)
W_{O3-30}	3.3	0.05	1.42	0.15	0.99	2.56
UV/W_{O3-30}	3.2	0.02	1.40	0.11	0.97	2.48
UV/TiO_2/W_{O3-30}	3.8	0.05	1.12	0.23	1.21	2.61

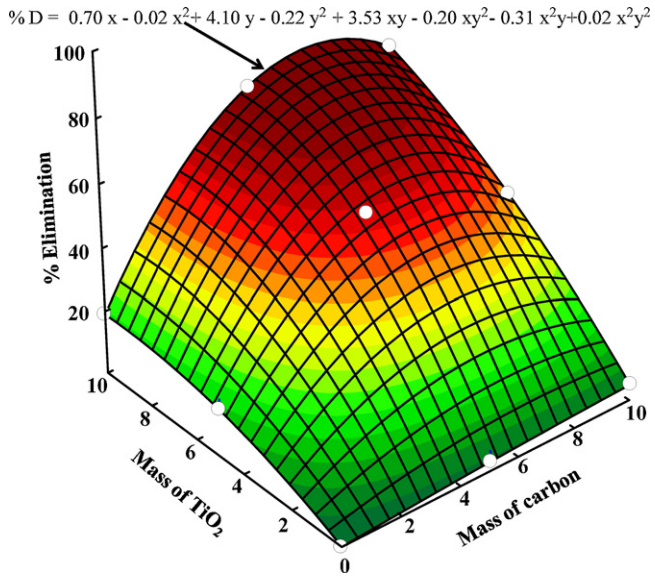

Fig. 5. Variation in percentage 2,4-D degradation by the UV/TiO_2/W_{O3-30} system with different masses of TiO_2 and activated carbon. T = 25 °C and pH 7, [2,4-D]$_0$ = 50 mg/L.

masses of carbon and TiO_2 as independent variables. The initial concentration of 2,4-D was 50 mg/L and the masses of carbon and TiO_2 were 0, 5, and 10 mg. The experimental response was fitted to the following equation:

$$\%\text{Degradation} = \beta_1 x + \beta_2 x^2 + \beta_3 y + \beta_4 y^2 + \beta_5 xy + \beta_6 xy^2 + \beta_7 x^2 y + \beta_8 x^2 y^2 \quad (7)$$

where, $\beta_1,\ldots,\beta_8$ are constants, x represents the carbon mass, and y is the TiO_2 mass. Carbon W_{O3-30} was selected for these experiments. Fig. 5 depicts the variation in percentage 2,4-D degradation as a function of the mass of TiO_2 and activated carbon. The percentage 2,4-D degradation in the presence of carbon or TiO_2 is very low and is markedly enhanced by increases in the mass of TiO_2 and carbon. Fig. 5 also shows that the highest percentage degradation was achieved with the addition of around 8 mg of both carbon and TiO_2.

3.4. 2,4-D photocatalytic degradation in the presence of radical scavengers

Radical species generated in the UV activation of TiO_2 may give rise to oxidation or reduction reactions.

$$TiO_2 + h\upsilon(UV) \rightarrow TiO_2(e_{CB}^- + h_{VB}^+) \quad (8)$$

$$TiO_2(h_{VB}^+) + H_2O \rightarrow TiO_2 + H^+ + HO^\bullet \quad (9)$$

$$TiO_2(h_{VB}^+) + OH^- \rightarrow TiO_2 + HO^\bullet \quad (10)$$

$$TiO_2(e_{CB}^-) + O_2 \rightarrow TiO_2 + O_2^{\bullet -} \quad (11)$$

$$TiO_2(e_{CB}^-) + H^+ \rightarrow TiO_2 + H^\bullet \quad (12)$$

In order to study which of these species are involved in 2,4-D degradation, experiments were conducted in the presence of radical scavengers (t-BuOH, CO_3^{2-}, or SO_4^{2-}). The reaction rate constant of these scavengers with e_{aq}^-, H• and HO• are given in Table 5.

Fig. 6 depicts the percentage 2,4-D degradation as a function of time with the UV/TiO_2/W_{O3-30} system in the presence of t-BuOH (1 M), SO_4^{2-}/CO_3^{2-} ions (1 M/1 M) and SO_4^{2-} ions (1 M). The percentage 2,4-D degradation after 60 min of treatment was 4%, 12%, and 38%, respectively. This figure also demonstrates that (i) radical H• participates in the 2,4-D photodegradation process, and (ii) the reduction in 2,4-D degradation rate is greater in the presence of t-BuOH (HO•, e_{aq}^-, and H• scavenger) than in the presence of SO_4^{2-}/CO_3^{2-} (HO• and e_{aq}^- scavenger) or SO_4^{2-} (e_{aq}^- scavenger) ions.

Table 5
Reaction rate constant of radical scavengers with e_{aq}^-, H• or HO• radicals [36].

Scavengers	$k_{e_{aq}^-}$ (L mol^{-1} s^{-1})	$k_{H^\bullet}$ (L mol^{-1} s^{-1})	$k_{HO^\bullet}$ (L mol^{-1} s^{-1})
CO_3^{2-}	3.5×10^5	–	3.9×10^8
SO_4^{2-}	1.0×10^6	–	–
t-BuOH	4.0×10^5	1.7×10^5	6.0×10^8

Based on the results in Fig. 6, we calculated the contribution of each radical species to the global 2,4-D degradation by the UV/TiO_2/W_{O3-30} system as a function of treatment time by subtracting the degradation kinetics corresponding to each radical from the overall degradation kinetics obtained by using the UV/TiO_2/W_{O3-30} system. The results are depicted in Fig. 7 and show that (i) the three radical species participate in the decomposition of 2,4-D throughout the treatment period, (ii) the contribution of H• to the global removal process increases initially and then remains constant after 30 min of treatment, (iii) the contribution of HO• radicals reduces initially and then remains constant after 30 min, and (iv) the contribution of e_{aq}^- increases initially and then remains virtually constant after 30 min.

Following the method reported above and using the same radical scavengers, we also studied the contribution of the different radicals to 2,4-D degradation with the UV/TiO_2 system, i.e., in the absence of activated carbon (results in Fig. 8). In contrast to

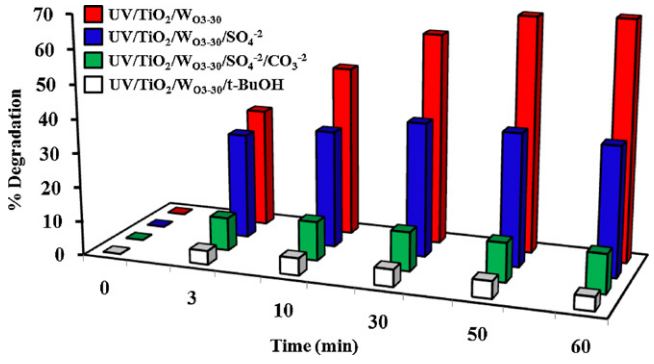

Fig. 6. 2,4-D degradation by the UV/TiO_2/W_{O3-30} system in the presence of radical scavengers, [t-BuOH]$_0$ = 1 M, [SO_4^{2-}]$_0$ = 1 M, and [SO_4^{2-}/CO_3^{2-}]$_0$ = 1 M/1 M. T = 25° C, pH 7, [2,4-D] = 50 mg/L, mass of TiO_2 and activated carbon = 5 mg, and V = 30 mL.

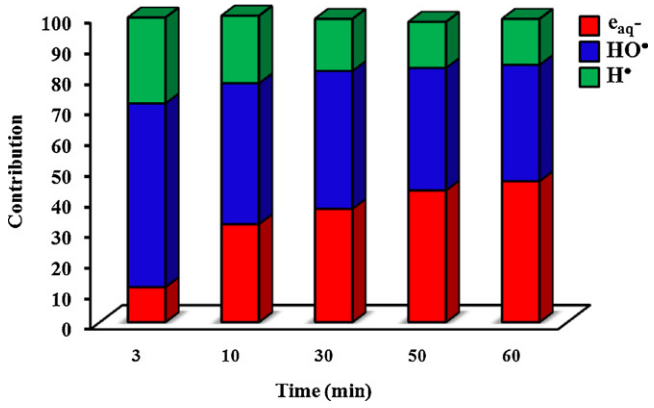

Fig. 7. Contribution of radical species to 2,4-D removal by the UV/TiO_2/W_{O3-30} system. T = 25 °C, pH 7, [2,4-D] = 50 mg/L, mass of TiO_2 and activated carbon = 5 mg.

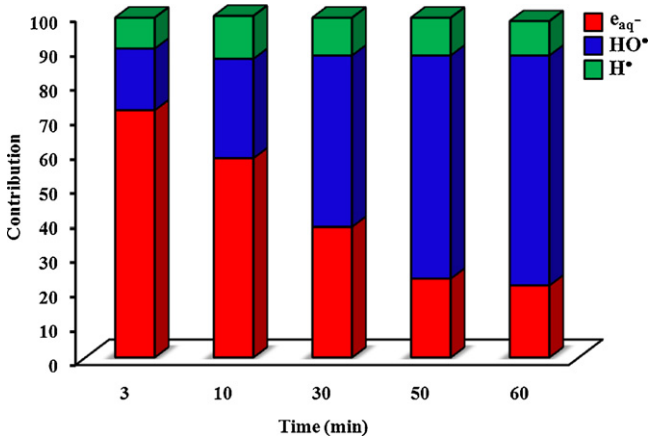

Fig. 8. Contribution of radical species to 2,4-D removal by the UV/TiO_2 system. T = 25 °C, pH 7, [2,4-D] = 50 mg/L, mass of TiO_2 and activated carbon = 5 mg.

observations in the presence of carbon W_{O3-30}, 70% of 2,4-D degradation was due to the contribution of electrons during the first 3 min, and this percentage gradually decreased until it reached 20% after 60 min, due to the higher contribution of HO• radicals.

The results shown in Figs. 7 and 8 again verify the action mechanism of ozonated carbons (reactions (1)–(3)) in the UV/TiO_2/activated carbon system, confirming the participation of the electrons initially generated in the production of HO• radicals when the UV/TiO_2/W_{O3-30} system was used.

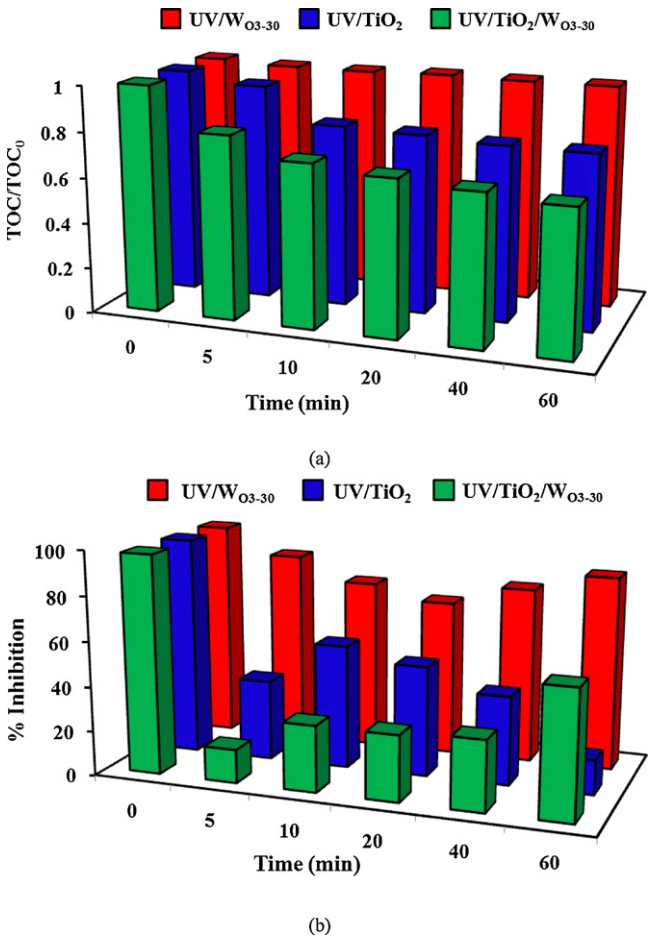

Fig. 9. Variation in (a) TOC and (b) toxicity during 2,4-D photodegradation with UV/TiO_2, UV/W_{O3-30}, and UV/TiO_2/W_{O3-30} systems. T = 25 °C, pH 7, [2,4-D] = 50 mg/L, mass of TiO_2 and activated carbon = 5 mg.

3.5. Time course of TOC and toxicity during 2,4-D degradation

Key aspects of the effectiveness of treatments of organic compound-polluted water are (i) the transformation of dissolved organic carbon into CO_2, and (ii) the toxicity of the degradation byproducts. We therefore studied these parameters during 2,4-D photodegradation.

Fig. 9a depicts the variation in TOC concentration as a function of treatment time. According to these results: (i) the UV/W_{O3-30} system does not markedly reduce the TOC, confirming the low adsorption capacity of the ozone-treated carbon; and (ii) the greatest percentage removal was achieved with the UV/TiO_2/W_{O3-30} system, due to the higher concentration in the medium of radical species, mainly HO• radicals.

Fig. 9b depicts the percentage inhibition of *Vibrio Fischeri* bacteria during 2,4-D photodegradation with UV/W_{O3-30}, UV/TiO_2, and UV/TiO_2/W_{O3-30} treatments. This percentage was 97% for the 2,4-D aqueous solution, demonstrating the high toxicity of 2,4-D, but it was drastically diminished with the UV/TiO_2, and UV/TiO_2/W_{O3-30} systems for 5 min o treatment, indicating that the degradation byproducts obtained have a lower toxicity in comparison to 2,4-D; however for longer treatment times the byproducts toxicity increased.

4. Conclusions

The presence of ozonated activated carbons with a high carboxyl groups content enhances 2,4-D photodegradation by the UV/TiO_2 system.

Carboxyl groups in the graphene planes of the activated carbon participate in the additional generation of HO• radicals by interacting with the electrons produced by the UV/TiO_2 system. Consequently, the contribution of HO• radicals to the global 2,4-D degradation process is greater at the beginning of the photocatalytic treatment.

The UV/TiO_2/W_{O3-30} system mineralized 40% of the organic matter present in the medium, and the toxicity of the degradation byproducts was considerably lower than that of 2,4-D.

Acknowledgements

The authors thank Dr. Rafael Robles for invaluable discussions on reaction mechanisms.

The authors are grateful for the financial support provided by MEC-DGI and FEDER (CTQ2011-29035-C02-02) and the Junta de Andalucía (RNM7522 and 3823).

References

[1] J. Hoigné, H. Bader, Water Research 10 (1976) 377–386.
[2] S.K. Kim, H. Chang, K. Cho, D.S. Kil, S.W. Cho, H.D. Jang, J. Choi, J. Choi, Materials Letters 65 (2011) 3330–3332.
[3] J. Gao, X. Luan, J. Wang, B. Wang, K. Li, Y. Li, P. Kang, G. Han, Desalination 268 (2011) 68–75.
[4] A.A. Ashkarran, S.A.A. Afshar, S.M. Aghigh, M. kavianipour, Polyhedron 29 (2010) 1370–1374.
[5] T. Ohno, F. Tanigawa, K. Fujihara, S. Izumi, M. Matsumura, Journal of Photochemistry and Photobiology A: Chemistry 118 (1998) 41–44.
[6] M. Faisal, S.B. Khan, M.M. Rahman, A. Jamal, K. Akhtar, M.M. Abdullah, Journal of Material Science and Technology 27 (2011) 594–600. 8.
[7] M. Antoniadou, V.M. Daskalaki, N. Balis, D.I. Kondarides, C. Kordulis, P. Lianos, Applied Catalysis B: Environmental 107 (2011) 188–196.
[8] R. Ocampo-Pérez, M. Sánchez-Polo, J. Rivera-Utrilla, R. Leyva-Ramos, Applied Catalysis B: Environmental 104 (2011) 177–184.
[9] R. Sellappan, J. Zhu, H. Fredriksson, R.S. Martins, M. Zäch, D. Chakarov, Journal of Molecular Catalysis A: Chemical 335 (2011) 136–144.
[10] C.G. Silva, J.L. Faria, Applied Catalysis B: Environmental 101 (2010) 81–89.

[11] F.J. Maldonado-Hódar, C. Moreno-Castilla, J. Rivera-Utrilla, Applied Catalysis A: General 203 (2000) 151–159.
[12] X. Wang, Y. Liu, Z. Hu, Y. Chen, W. Liu, G. Zhao, The Journal of Hazardous Materials 169 (2009) 1061–1067.
[13] G. Xue, H. Liu, Q. Chen, C. Hills, M. Tyrer, F. Innocent, The Journal of Hazardous Materials 186 (2011) 765–772.
[14] W. Wang, C.G. Silva, J.L. Faria, Applied Catalysis B: Environmental 70 (2007) 470–478.
[15] Y. Li, X. Li, J. Li, J. Yin, Catalysis Communications 6 (2005) 650–655.
[16] J. Matos, J. Laine, J. Herrmann, Journal of Catalysis 200 (2001) 10–20.
[17] T. Cordero, C. Duchamp, J. Chovelon, C. Ferronato, J. Matos, Journal of Photochemistry and Photobiology A: Chemistry 191 (2007) 122–131.
[18] D. Han, W. Jia, H. Liang, Journal of Environmental Sciences 22 (2010) 237–241.
[19] Z. Aksu, E. Kabasakal, Separation and Purification Technology 35 (2004) 223–240.
[20] A.J. Gold, T.G. Morton, W.M. Sullivan, J. Mcclory, Water Air Soil Pollution 37 (1988) 121–129.
[21] D.D. Leavitt, M.A. Abraham, Environmental Science Technology 24 (1990) 566–571.
[22] W.A. Jury, D.D. Focht, W.J. Farmer, Journal of Environmental Quality 16 (1987) 422–428.
[23] E. Piera, J.C. Calpe, E. Brillas, X. Domènech, J. Peral, Applied Catalysis B: Environmental 27 (2000) 169–177.
[24] M.I. Bautista-Toledo, J.D. Méndez-Díaz, M. Sánchez-Polo, J. Rivera-Utrilla, M.A. Ferro-García, Journal of Colloid and Interface Science 317 (2008) 11–17.
[25] M. Sánchez-Polo, J. Rivera-Utrilla, Carbon 41 (2003) 303–307.
[26] V.L.K. Jennings, M.H. Rayner-Brandes, D.J. Bird, Water Research 35 (2001) 3448–3456.
[27] I.T. Cousins, C.A. Staples, G.M. Kelecka, G.M. Mackay, Human and Ecological Risk Assessment 8 (2002) 1107–1135.
[28] M. Sánchez-Polo, J. Rivera-Utrilla, G. Prados-Joya, M.A. Ferro-García, I. Bautista-Toledo, Water Research 42 (2008) 4163–4171.
[29] J. Rivera-Utrilla, Water Research 41 (2007) 2480.
[30] M. Sánchez-Polo, J. Rivera-Utrilla, J.D. Méndez-Díaz, S. Canonica, U. von Gunten, Chemosphere 68 (2007) 1814–1820.
[31] J. Rivera-Utrilla, M. Sánchez-Polo, Carbon 40 (2002) 2685–2691.
[32] R. Ocampo-Perez, R. Leyva-Ramos, J. Mendoza-Barron, R.M. Guerrero-Coronado, Journal of Colloid and Interface Science 364 (2011) 195–204.
[33] R. Ocampo-Perez, R. Leyva-Ramos, P. Alonso-Davila, J. Rivera-Utrilla, M. Sanchez-Polo, Chemical Engineering Journal 165 (2010) 133–141.
[34] H. Valdés, M. Sánchez-Polo, J. Rivera-Utrilla, C.A. Zaror, Langmuir 18 (2002) 2111–2116.
[35] L.E. Depero, L. Sangaletti, B. Allieri, E. Botempi, R. Salari, M. Zocchi, C. Casale, M. Notaro, Journal of Materials Research 13 (1998) 1644–1649.
[36] B.R. Buxton, C.L. Greenstock, W.P. Helman, A.B. Ross, Journal of Physical and Chemical Reference Data 17 (1988) 513–886.